Muon diffusion and spin dynamics in copper

G. M. Luke,* J. H. Brewer, S. R. Kreitzman, and D. R. Noakes[†]

Department of Physics, University of British Columbia, Vancouver, Canada V6T 2A3

M. Celio[‡] and R. Kadono[§]

TRIUMF, 4004 Wesbrook Mall, Vancouver, Canada V6T 2A3

E. J. Ansaldo

Department of Physics, University of Saskatchewan, Saskatoon, Canada S7N 0W0

(Received 29 August 1990)

We have studied the quantum diffusion of positive muons in pure copper over the temperature range 12 mK $\leq T \leq$ 150 K using the technique of muon-spin relaxation. The rate of diffusion has been deduced from its effect upon the muon-polarization function. The measurements were made in a weak longitudinal external magnetic field, where the spin relaxation has proved to be the most sensitive to the muon hop rate below 150 K. Our results for the behavior of the muon hop rate are well explained by the recently developed theories for the quantum diffusion of light interstitials in metals by Kondo, Yamada, and others. These theories stress the effects of the conduction electrons in the metal in providing a form of "friction," retarding the diffusion process. In addition, we have utilized the technique of level-crossing resonance spectroscopy, by measuring the electric-quadrupole interaction strength of the copper nuclei. These results have enabled us to show that the muon occupies the same octahedral site at all the temperatures studied, ruling out the possibility of metastable muon sites contributing to any significant portion of the muon polarization in the temperature range studied.

I. INTRODUCTION

The study of the diffusion of light interstitials in metals has generated considerable theoretical and experimental interest, primarily because various quantum effects are expected and have, in fact, been observed. Light interstitials are also the most likely to exhibit anomalous behavior at low temperatures, as a result of their low mass. The field of hydrogen in metals has been extensively studied; hydrogen isotopes diffuse the most quickly of all atomic interstitials and offer a wide range of masses (factor of 3) with which to test theories of diffusion processes. In addition, hydrogen isotopes are the simplest impurities and therefore the most tractable theoretically. The positive muon μ^+, with its mass approximately $\frac{1}{9}$ that of a proton, can also be implanted into metals, extending the mass range of hydrogenlike impurities an order of magnitude lower. As a result of its low mass, the muon provides a particularly severe test for theories of quantum diffusion.

The first measurements of muon diffusion in metals were made by Gurevich *et al.*[1] and Grebinnik *et al.*[2] in transverse field (TF). The muon hop rate was deduced through the motional narrowing it caused of the TF muon-spin relaxation. They found that the muon hop rate decreased with decreasing temperature, following an Arrhenius-like temperature dependence. The spin relaxation rate became constant below 80 K (down to 20 K), which they took as evidence that the muons were static

at low temperatures. The size of the activation energy they obtained was such that the diffusion process was taken to be that of thermally activated tunneling.

The orientational and field dependence of the transverse-field relaxation[3] was used to identify the muon site in the lattice. This site, located at the center of a copper octahedron, is shown in Figure 1. Subsequent TF measurements[4-6] at temperatures below 20 K found that
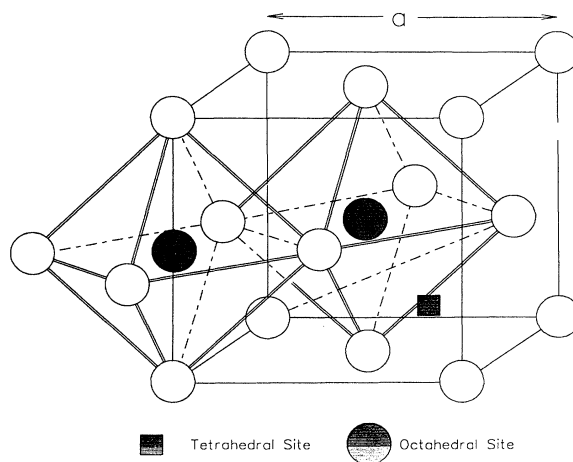
FIG. 1. The muon site in the copper lattice at the center of a copper octahedron. Also shown is the tetrahedral site, proposed by several authors.

the muon-spin relaxation rate started to decrease again with decreasing temperature. The most likely interpretation was an increase in the muon hop rate with decreasing temperature, causing motional narrowing as at higher temperatures. The field and orientation dependence of the relaxation rate were consistent with an unchanged octahedral muon site, with an unchanged electric-field gradient, implying that the decreased depolarization rate was in fact due to increased hopping between such sites.

There were, however, a number of other possible effects that could not be distinguished in the transverse-field measurements from an increase in the hop rate. This was because it is difficult to distinguish changes in the depolarization rate due to changes in the correlation time $\tau_c \sim 1/\nu_{hop}$ from changes due to a smaller static relaxation rate σ. Some of these possibilities included the muon moving to a different site in the lattice, perhaps the tetrahedral site (also shown in Fig. 1), as well as trapping at defects or impurities. The latter were investigated by deliberately introducing defects into samples, through radiation damage[7] and by mechanical deformation to introduce dislocations.[8] In both experiments, the introduction of large numbers of defects did not appreciably alter the TF relaxation rate, implying that the small number of these defects present in annealed crystals and polycrystals could not be responsible for the changes with temperature of the relaxation rate (and thus the inferred muon hop rate). Experiments on isotopically enriched samples containing over 99% of either ^{63}Cu or ^{65}Cu also yielded essentially the same results as the natural composition samples.[5,6]

The narrowing was studied down to 50 mK;[5,6] the hop rate was observed to reach a plateau at approximately 500 mK, below which it remained constant. The authors claimed to be able to rule out a number of models that proposed alternate explanations for the effects on the relaxation functions, including metastable tetrahedral site occupation and trapping at impurities, and concluded that the diffusion was due to a coherent tunneling process. However, the TF experiments were not sufficient to completely rule out all other interpretations.

Zero-field (ZF) measurements[9−12] all exhibit a minimum in the muon hop rate around 40 K. There is a large variation in the absolute (fitted) value of the hop rate at this minimum, however, due to the difficulty in extracting very small hop rates from ZF data. The most recent results of Kadono et al.[12,11] indicate that muons are completely static ($\nu_{hop} = 0 \pm 10^{-2}$ μs^{-1}) around 40 K. The actual range extracted for static behavior was found to vary with the form of the static depolarization function used to fit the data. Use of the semiclassical Kubo-Toyabe[13,14] function resulted in a static range from 20 to 80 K, whereas use of the more accurate results of Celio and Meier[15] gave a narrower range of temperatures. Earlier results[16,9] gave the value of ν_{hop} at the minimum as $\sim 10^{-1}$ μs^{-1}.

At higher temperatures (100 K and higher) the hop rates extracted from the ZF data are consistent with each other, as well as with the various TF results[1,2,17] up to

~ 140 K.

Below the minimum, an increasing hop rate was seen, down to 0.5 K. The hop rate was seen to obey a power law in this range of the form

$$\nu_{hop} \sim T^{-\alpha}, \tag{1}$$

where values for the exponent varied from $\alpha \sim 0.4$ (Ref. 16) to $\alpha = 0.67 \pm 0.03$ in the most recent results.[11] The value of α depended on the range of temperatures used to extract it; with deviations from the power law starting at around 0.5 and 15 K. Below T=0.5 K the hop rate was observed to level out, reaching a constant value in the range 0.5-0.8 μs^{-1}. These ZF measurements were made down to ~ 70 mK.

Our preliminary weak longitudinal field[18,19] (WLF) results were in qualitative agreement with the previous TF and ZF work, and demonstrated the precision of the WLF technique. Here we present our final results for the muon diffusion rate over the temperature range 12 mK $\leq$ T $\leq$ 150 K. All of the data are analyzed in terms of an exactly solved, fully quantum-mechanical microscopic Hamiltonian governing the time evolution of the muon polarization in the absence of diffusion. The effects of muon diffusion are then extracted from the data using the strong collision model.[20,14]

This article proceeds as follows. First, there is a discussion of the evaluation of muon relaxation functions, for the case of static models. These static relaxation functions are then used to extract the strength of the muon-nuclear quadrupolar interaction, which allows the determination of the muon site. This is then followed by a description of the strong collision model, used to extract the muon hop rate. Finally, the temperature dependence of the muon hop rate is compared to the theoretical results of Kondo, Yamada, and others.

II. RELAXATION FUNCTIONS

The semiclassical theory of Kubo, Toyabe, and co-workers[13,14] gives an approximate method for evaluating the time evolution of a classical spin ensemble in zero and longitudinal field. The local fields are taken to be static and random with a Gaussian distribution:

$$P(H_i) = \frac{\gamma_\mu}{\sqrt{2\pi}\Delta} \exp\left(\frac{-\gamma_\mu^2 H_i^2}{2\Delta^2}\right), \quad i = x, y, z, \tag{2}$$

which has a second moment given by the dipolar width Δ

$$\frac{\Delta^2}{\gamma_\mu^2} = \langle H_x^2 \rangle = \langle H_y^2 \rangle = \langle H_z^2 \rangle. \tag{3}$$

The spin evolution function is found by integrating over the field distributions in all three dimensions. The result is the well-known Kubo-Toyabe formula for the evolution of a static spin in zero field:

$$\mathcal{P}_z(t) = \frac{1}{3} + \frac{2}{3}(1 - \Delta^2 t^2)\exp(-\frac{1}{2}\Delta^2 t^2). \tag{4}$$

The "$\frac{1}{3}$ tail" corresponds to the fraction of the spin po-

larization, which has its random local field aligned either parallel or antiparallel with its initial polarization, while the remaining $\frac{2}{3}$ of the polarization precesses in the transverse local field components.

The above procedure is easily generalized to include an external longitudinal field, with the result that the long-time asymptotic value of the polarization increases from $\frac{1}{3}$ towards 1.

Although useful in that it is a simple model that displays approximately correct behavior, Kubo-Toyabe theory is not precise enough to permit accurate measurement of subtle differences from the static relaxation functions. Therefore, we have calculated theoretical muon-spin polarization functions following the method of Celio.[21] This technique allows us to exactly solve the spin Hamiltonian for the muon interacting with its six nearest-neighbor copper nuclei, including the nuclear dipolar interaction, the nuclear quadrupolar interaction between the copper nuclei and the electric-field gradient induced by the muon, as well as the Zeeman interactions of the muon and the copper nuclei. The only interaction that is neglected is the dipolar interaction between copper nuclei, whose effect is negligible in the time range of interest. In general, the spin Hamiltonian is given by

$$\mathcal{H}_{\text{tot}} = \sum_{i=1}^{N} \mathcal{H}_i, \quad [\mathcal{H}_i, \mathcal{H}_j] \neq 0 \quad \text{for } i \neq j \tag{5}$$

where each term in the sum over N neighbors is the sum of dipolar, quadrupolar, and Zeeman terms:

$$\mathcal{H}_i = \mathcal{H}_i^D + \mathcal{H}_i^Q + \mathcal{H}_i^Z, \tag{6}$$

where, in terms of the muon spin $\mathbf{I}$ and the nuclear spins $\mathbf{J}_i$ and the muon-nuclear vector $\mathbf{n}_i$:

$$\mathcal{H}^Z = \frac{1}{N} \hbar \gamma_\mu \mathbf{I} \cdot \mathbf{B} - \hbar \gamma_{\text{Cu}} \mathbf{J}_i \cdot \mathbf{B} \tag{7}$$

$$\mathcal{H}_i^D = \hbar \omega_i^D [\mathbf{I} \cdot \mathbf{J}_i - 3(\mathbf{I} \cdot \mathbf{n}_i)(\mathbf{J}_i \cdot \mathbf{n}_i)] \tag{8}$$

$$\mathcal{H}_i^Q = \hbar \omega^Q [(\mathbf{n}_i \cdot \mathbf{J}_i)(\mathbf{n}_i \cdot \mathbf{J}_i) - J(J+1)/3]. \tag{9}$$

The quadrupolar term arises from the fact that the muon destroys the cubic symmetry of its neighboring copper nuclei and exerts an electric field on them. It is assumed in Eq. (9) that the electric-field gradient on each copper nucleus is axially symmetric around $\mathbf{n}_i$ and is the only field gradient present. The quadrupolar frequency ω^Q is given in terms of the quadrupole moment of the nucleus Q and the electric-field gradient (EFG) eq by

$$\hbar \omega^Q = \frac{3e^2 qQ}{4J(2J-1)}. \tag{10}$$

As the electric-field gradient and the muon-nuclear separation are dependent on the local geometry, the quadrupolar frequency will depend on the muon site.

The muon polarization is the quantity measured; in terms of the density matrix ρ, it is

$$\mathcal{P}_\mu(t) = \text{Tr}[\rho \sigma_\mu(t)], \tag{11}$$

where the density matrix ρ is given in terms of the Pauli matrices $\sigma_\mu = 2\mathbf{I}_\mu$. Celio uses the Trotter formula to evaluate the time development of the spin states:

$$|\psi_n(t)\rangle = \lim_{k \to \infty} \left(\prod_{j=1}^{N} \exp[-\mathcal{H}_j(t)/\hbar k] \right)^k |\psi_n(0)\rangle. \tag{12}$$

The advantage of this procedure is that each of the $\mathcal{H}_j$ describes the interaction of a single nuclear spin $\mathbf{J}_j$ with that of the muon and as a result have the simple structure $\mathbb{1}_1 \otimes \mathbb{1}_2 \cdots \otimes \mathcal{H}_j \otimes \cdots \otimes \mathbb{1}_N$, where $\mathbb{1}$ is the unit matrix. For a muon sitting in an octahedral interstitial site (as for the case of copper), this procedure allows one to consider only the 8×8 portions of the Hamiltonian corresponding to the interaction of the muon with one of its spin-$\frac{3}{2}$ neighbors. The problem of diagonalizing a large (8192×8192) matrix has been replaced by a large number of multiplications of much smaller ones. In practice, the largest value of k in Eq. (12) is chosen such that any error in the resulting polarization is negligible over the time region of interest (usually $t < 16$ μs).

Rather than follow this procedure for all 4096 (for a polarized muon interacting with six copper nuclei) possible initial states, one chooses a random set of a_i's, subject to normalization conditions, and repeats this time development a number of times, averaging over the final result. The accuracy of this random-phase approximation increases with the dimensionality of the spin system and the number of times the calculation is performed for different initial states.

We calculated theoretical relaxation functions for polycrystalline samples by repeating the entire procedure for a number (typically 10) of different random orientations of the crystalline axes, averaging over the result.

Figure 2 shows a set of calculated relaxation functions
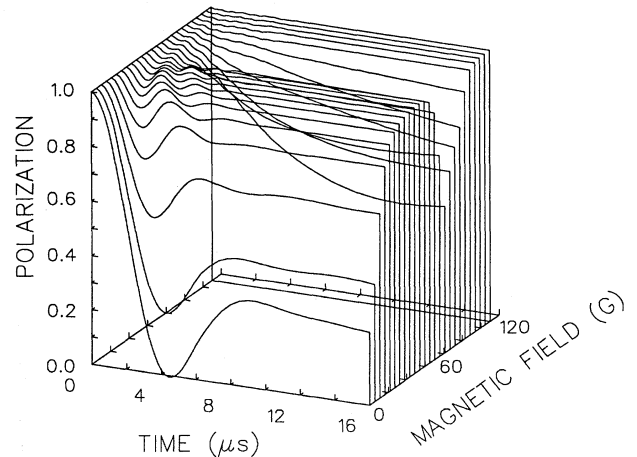
FIG. 2.   Exact muon-polarization function: six nearest-neighbor Cu atoms, for longitudinal fields between $0 \to 120$ G, applied along the $\langle 111 \rangle$ direction.

for various longitudinal fields from 0 to 120 G. One of the striking features of Fig. 2 is the enhanced relaxation which occurs around $B_{\text{res}} \approx 80$ G. This level-crossing resonance (LCR) occurs[22] when the quadrupolar splitting of the muon's nearest-neighbor copper nuclei is approximately equal to the muon's Zeeman splitting. At this field, the dipolar coupling between the spins causes a cross relaxation to take place, as energy-conserving flip-flop transitions can occur.

The resonance effect can be demonstrated by considering the simple case of a muon interacting with a single spin-$\frac{3}{2}$ copper nucleus with the external magnetic field applied along the $\hat{z}$ direction. In general, for applied fields greater than the dipolar field of approximately 4 G, the Hamiltonian is essentially diagonal in the direct product representation of muon spin I_z and copper spin J_z, as the diagonal elements of the Hamiltonian are much larger than the off-diagonal ones. This means that there are very few transitions between states with different muon spin, and there is little relaxation of the muon asymmetry. However, near the field where the muon Zeeman frequency equals the copper quadrupole frequency, the diagonal elements become very small, and there is a large mixing of states; the initial state is no longer an eigenstate. Transitions to other states with a different $\hat{z}$ component of the muon spin are enhanced, and there is an increased muon-spin depolarization.

The copper energy levels are also split by the nuclear Zeeman interaction. As a result, the resonance (for a muon and a single copper nucleus) is a superposition of four lines, whose positions and relative amplitudes depend on the orientation angle θ (between the muon-nuclear axis and the applied field). The width of each individual line is given by the strength of the coupling between the mixing states, i.e., the dipolar field of approximately 4 G. The actual positions of the lines will be distributed over a field range of the order of the copper nuclear Zeeman interaction strength ($B_{\text{res}}\gamma_{\text{Cu}}/\gamma_{\mu} \sim 20$ G). For a larger number of nuclei (six for the muon in the octahedral site), the resonance contains contributions from copper nuclei at a number of different angles, which are convolved together in a complicated manner. The individual lines are not resolved, as their separation is less than their linewidth; the total width of the resonance is still of the order of the copper nuclear Zeeman strength. A further source of broadening is due to the copper isotope mixture (^{63}Cu/^{65}Cu), though this contribution is smaller than that of the nuclear Zeeman interaction.

The LCR provides an extremely sensitive indicator of the muon site, since its position is determined by the strength of the EFG exerted on the copper nuclei. If the muon were to occupy a different site, with a different muon-copper separation, the position of the resonance would shift. Additionally, the number of nuclei involved in the resonance would change, and there would be a change in the form of the relaxation function, even if the muon-nuclear distance remained the same. An illustration of this sensitivity of the LCR technique to the

detailed nature of the muon site has been its use in proving that the so-called "anomalous" muonium center in silicon is situated exactly between two silicon nuclei.[23]

III. STRONG COLLISION MODEL FOR DIFFUSION

The above discussion has been restricted to the case where the muon is static, i.e., fixed at one site in the lattice. If the muon is diffusing, however, the relaxation of the μ^+ polarization will be modified, as it hops from one site—where it has exchanged some of its polarization with its neighbors—to another site, surrounded by initially unpolarized nuclei. The effects of diffusion are generally described within the framework of the strong collision model.[20,14,24] The term "strong collision" refers to the evolution of the local field experienced by the μ^+, which is assumed to change discontinuously at the time of a hop and to be uncorrelated with the evolution at the previous site.

In the strong collision model the muon is assumed to be hopping at random times between equivalent sites, with some average frequency ν. The time spent during a jump is taken to be much shorter than the mean residence time at a site. The probability that the muon is still at its initial site after some period of time is simply given by an exponential decay:

$$P \text{ (at initial site)} = e^{-\nu t}. \tag{13}$$

The model also assumes that there is no correlation between the local field experienced by the muon before and after a hop (other than external fields). Thus the correlation of the local field at some site j at time t with that at time 0 and site i is given by

$$\langle H_i(0)H_j(t)\rangle = \delta_{ij}\langle H_i^2(0)\rangle e^{-\nu t}. \tag{14}$$

The muon polarization at some time t will then contain contributions from muons that have not hopped at all, those that have hopped once, twice, and so on:

$$\mathcal{P}_z(t) = \sum_{n=0}^{\infty} \rho_z^{(n)}(t), \quad \text{where n= number of hops} \tag{15}$$

$$= e^{-\nu t}[\rho_z(t)$$

$$+ \nu \int_0^t \rho_z(t_1)\rho_z(t-t_1)dt_1$$

$$+ \nu^2 \int_0^t \int_0^{t_1} \rho_z(t_1)\rho_z(t_2-t_1)\rho_z(t-t_2)dt_1 dt_2$$

$$+ \cdots]. \tag{16}$$

This can be solved by taking the Laplace transform and summing the infinite series, giving a result that can be inverted numerically. Equation (16) can be expressed as

$$\mathcal{P}_z(t) = e^{-\nu t}\rho_z(t) + \nu \int_0^t \rho_z(\tau)e^{-\nu\tau}\mathcal{P}_z(t-\tau)d\tau. \tag{17}$$

This expression can be solved by numerical integration, allowing one to generate "dynamic" relaxation functions from static ones, as a function of the average hop rate. Figures 3 and 4 show theoretical relaxation functions for both zero field and weak longitudinal field for several hop rates.

In zero field, there are two simple limits where the form of the relaxation function can be illustrated. In the case of slow hopping and long times, where the mean hop frequency is much smaller than the second moment of the field distribution (i.e., Δ in Kubo-Toyabe theory) and the time is much longer than $1/\Delta$, the effects of hopping are seen in the $\frac{1}{3}$ tail, which decays slowly:

$$\mathcal{P}_z(t) \simeq \frac{1}{3}\exp\left(\frac{-2}{3}\nu t\right) \quad (\nu \ll \Delta, \ t \gg \Delta^{-1}). \quad (18)$$

In this limit, the decay of the tail becomes independent of Δ, whose value can be deduced from the second moment of the polarization (i.e., from short times), which is independent of the hop rate. Most of the muons do not hop until times longer than the time at which the polarization has reached its minimum value (at $t \sim \sqrt{3}/\Delta$) and begun its recovery towards its static asymptotic value of $\frac{1}{3}$. Thus the minimum remains, with the main effect of slow hopping being the relaxation of the tail at long times.

In the limit of fast hopping, where the hop rate is much larger than Δ but still smaller than the dominant energy splittings in the system (such as Zeeman or quadrupole), one finds that the relaxation function has the form

$$\mathcal{P}_z(t) \simeq \exp\left(\frac{-2\Delta^2 t}{\nu}\right) \quad (\Delta \ll \nu \ll \gamma_I H_z, \omega^Q). \quad (19)$$

This corresponds to the extreme motional narrowing limit, at hop rates that are past the "T_1 minimum." The minimum in the relaxation function disappears, as the majority of the muons hop before the polarization reaches its minimum (at $t_{\min} \sim \sqrt{3}/\Delta$), which is therefore never reached.
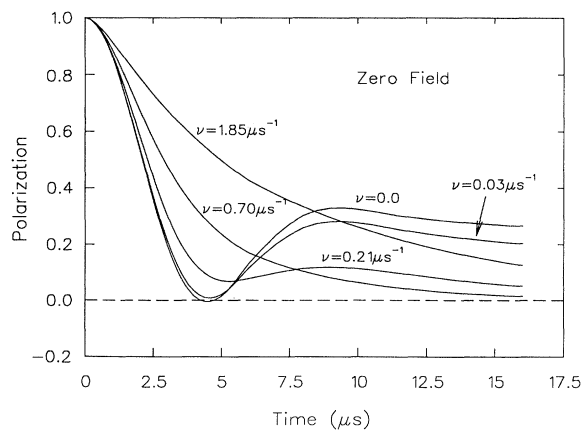
The effect of diffusion on the relaxation function in copper is shown in Fig. 3 for zero field and in Fig. 4 for weak longitudinal field. In zero field and at low hop rates there is little change in the relaxation function until long times ($t > 8\ \mu$s), whereas in WLF the changes occur much earlier. This difference makes the WLF method more sensitive in measuring very small hop rates.

There are a number of experimental situations where some of the assumptions of the strong collision model could be violated and thus the model could be expected to break down. First, the assumption that the local fields experienced by the diffusing particle before and after hopping are uncorrelated does not hold in the case of back diffusion (where the particle hops from one site and then returns to its original site). Second, there is the case of shared neighbors, before and after hopping. Celio[25] considered these effects in a number of numerical simulations of worst-case situations. He found that the general result of the correlations was to modify the extracted value of the hop rate by some constant factor (i.e., independent of the hop rate) of order 1.

IV. DIFFUSION OF LIGHT INTERSTITIALS

In considering the diffusion of light interstitials, one must account for the effects of the host material acting to retard the motion of the diffusing particle. Flynn and Stoneham[26] first considered the effects of the self-trapping lattice distortion around the particle acting to reduce the effective tunneling matrix element from its bare value $\mathcal{J}_0$:

$$\mathcal{J}_{\text{eff}} = \mathcal{J}_0 \exp[-S(T)] \quad (20)$$

where $S(T)$ depends upon the phonons in the system, giving at low temperatures a T^7 temperature dependence on the hop rate $\mathcal{W}$ (which is proportional to $\mathcal{J}_{\text{eff}}^2$). Kagan and Klinger[27] extended the theory to include a quadratic interaction between the diffusing particle and the host

FIG. 3. Muon polarization in zero field (ZF) for several muon hop rates, calculated from static relaxation function using the strong collision model.
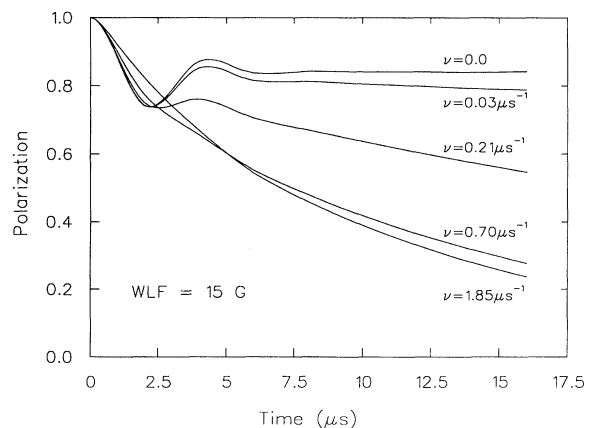
FIG. 4. Muon-polarization function in weak longitudinal field (WLF) at several muon hop rates, calculated using the strong collision model.

lattice and predicted a T^{-9} dependence at sufficiently low temperatures.

Kondo[28] and Yamada[29] considered the important effect of the conduction electron cloud on the motion of the diffusing particle. In a metal, there exist infinitely small electron excitations across the Fermi level, with the result that the conduction electrons react slowly to perturbations and therefore cannot follow the diffusing particle adiabatically. Since the conduction electron cloud must follow the charged diffusing particle, this effect causes a source of "drag," reducing the particle hop rate.

Kondo finds that at sufficiently low temperatures, the hop rate is given by

$$W = \frac{\mathcal{J}_0^2 e^{-2S}}{\varepsilon_F} \sqrt{\pi} \frac{\Gamma(K)}{\Gamma(K + \frac{1}{2})} \left(\frac{\pi k_B T}{\varepsilon_F} \right)^{2K-1} \quad (21)$$

where Γ is the gamma function, ε_F is the Fermi energy, and S is the zero-temperature value of $S(T)$. The constant K is a measure of the particle-conduction electron interaction strength. The factor of T^{2K} is from the electron cloud and reflects the near orthogonality of the conduction-electron wave functions at the two sites (before and after hopping), reducing the overlap integral. The T^{-1} factor comes from the fact that the energy levels become sharper (with the level broadening being proportional to temperature) with decreasing temperature, and thus the overlap integral increases correspondingly. Equivalently, the final electron density of states is reduced by the smearing of the Fermi surface, which is proportional to T.

At this point Kondo considers the further effect of a temperature-independent inhomogeneous broadening of the hopping particle energy levels,[28] characterized by a width δ_E. As a result, below $T \sim \delta_E$, the energy levels no longer become sharper with decreasing temperature and at temperatures much lower than δ_E the hop rate exhibits only the T^{2K} temperature dependence; the hop rate starts to decrease again with decreasing temperature.

The hop rate is evaluated numerically as a function of the microscopic parameters describing the various interactions: the linear and quadratic particle-lattice interactions (S and d), the bare tunneling matrix element ($\mathcal{J}_0$), the particle-conduction electron interaction (K), the Debye temperature (Θ_D), Fermi energy (ε_F), inhomogeneous broadening (δ_E), and the temperature T:

$$W = \frac{\mathcal{J}_0^2}{\Theta_D} \Xi \left(\frac{T}{\Theta_D}, S, K, \frac{\varepsilon_F}{k_B \Theta_D}, d, \frac{\delta_E}{\Theta_D} \right). \quad (22)$$

Comparison with the measured results for $W(T)$ allows the determination of these various microscopic parameters.

V. EXPERIMENTAL

The technique of muon-spin relaxation (μSR) has been described in detail in a number of books[30] and conference proceedings,[31] and so only a brief description will

be given here. A μSR experiment involves the implanting, generally one at a time, of highly polarized positive muons. The muon comes to rest in the target and samples the local magnetic environment through its spin. After some length of time the muon decays, emitting two neutrinos (which are not observed) and a positron that is detected in another scintillation counter. The angular distribution of the decay positrons is monitored to give information on how the muon spin evolved before the decay.

A. Time-differential (TD) μSR

Typically, a muon enters the sample after passing through a thin scintillation counter, which signals the start of an event. For each detector, a histogram of detected positrons is kept as a function of the time difference between when the muon enters the sample and when it decays. The numbers of positrons detected in two opposing counters (say F and B, for the forward and backward directions) are given by

$$N_B(t) = N_0^B \{ B_B + e^{-t/\tau_\mu} [1 - A_0^B \mathcal{P}(t)] \},$$

$$N_F(t) = N_0^F \{ B_F + e^{-t/\tau_\mu} [1 + A_0^F \mathcal{P}(t)] \}, \quad (23)$$

where B_B, F_B correspond to the fraction of time-independent background events, A_0^B, A_0^F are the asymmetries of the B and F counters and $\mathcal{P}$ is the muon polarization function discussed in the previous section. An experimental asymmetry is then defined:

$$\mathcal{A}(t) \equiv \frac{\mathcal{B}(t) - \mathcal{F}(t)}{\mathcal{B}(t) + \mathcal{F}(t)}. \quad (24)$$

This can be inverted to give the corrected asymmetry:

$$A_0^B \mathcal{P}(t) = \frac{(\alpha - 1) + (\alpha + 1)\mathcal{A}(t)}{(\alpha\beta + 1) + (\alpha\beta - 1)\mathcal{A}(t)}, \quad (25)$$

where

$$\alpha \equiv \frac{N_0^F}{N_0^B}, \quad \beta \equiv \frac{A_0^F}{A_0^B}, \quad (26)$$

which equals $\mathcal{A}(t)$ when $\alpha = \beta = 1$.

In the zero or longitudinal field (ZF-LF) geometry, the muon spins are initially polarized normal to the planes of the (F and B) positron detectors, along the direction of the applied field (in a LF experiment).

B. Time-integral μSR

It is not always necessary to completely determine the entire muon-polarization function. In some instances it is sufficient to measure only its average value (weighted by the distribution of μ^+ decay times) over some length of time, long relative to the muon lifetime. In this case, one is no longer restricted to allowing only one muon in the sample at a time. This allows the use of greatly increased muon beam intensities, which provides increased

sensitivity in some types of experiments.

In a time-integral μSR experiment one simply counts all the decay positrons in each detector. After a period of time T, much longer than the muon lifetime τ_μ, the number of decay positrons detected is given by

$$\mathcal{N}_\pm = B_\pm T + RT\epsilon_\pm + RT\epsilon_\pm A_\pm \mathcal{L}(\mathcal{P}_z), \qquad (27)$$

where R is the muon arrival rate, ϵ is the efficiency, B is the background rate, and A is the effective asymmetry of the positron detector. The $\pm$ refers to the counter direction relative to the initial muon polarization. Only the LF-ZF geometry is presently considered useful for integral μSR measurements. Here, $\mathcal{L}(\mathcal{P}_z)$ is the Laplace transform of $\mathcal{P}_z(t)$ defined by

$$\mathcal{L}(\mathcal{P}_z) = \int_0^\infty \exp(-t/\tau_\mu)\mathcal{P}_z(t)dt/\tau_\mu. \qquad (28)$$

One can then form an integrated asymmetry

$$\mathcal{A}_{\text{int}} \equiv \frac{\mathcal{N}_+ - \mathcal{N}_-}{\mathcal{N}_+ + \mathcal{N}_-}. \qquad (29)$$

If the counters are essentially identical,

$$\mathcal{A}_{\text{int}} \approx \frac{(1-\alpha)}{(1+\alpha)} + \frac{2}{(1+\alpha)}A\mathcal{L}(\mathcal{P}_z), \qquad (30)$$

where α is the ratio of the counter efficiencies [given in Eq. (26)]. The first term is a "baseline," which is generally both field-dependent and rate-dependent, while the second contains the signal of interest.

C. Experimental details

The experiments were performed on the M15 and M20B surface muon channels at the TRIUMF meson factory. These channels provide monochromatic beams of $\sim$ 100% spin-polarized muons with a momentum of approximately 28 MeV/c. Such muons have a range of about 150 mg/cm^2, corresponding to about 0.1 mm in copper. Beam positrons were removed from the beam using a dc separator (consisting of crossed electric and magnetic fields).

Above 4 K, the samples were mounted in a He flow cold finger cryostat. Measurements below 4 K were performed using a commercial (Oxford model 400) top-loading dilution refrigerator, which had a base temperature of 10 mK. The various cryostats were fitted with thin Mylar or Kapton windows to allow beam access. When using the cold finger cryostat, the samples were first attached to a piece of high purity aluminum using low-temperature varnish. This aluminum was then bolted to the cold finger using a thin layer of Apiezon N-type grease for improved thermal contact. Nonsuperconducting solder was used for mounting the sample to the dilution refrigerator sample holder, which was attached to the mixing chamber extension using a threaded copper contact.

Temperature measurement was made using carbon glass and platinum resistors in the cold finger cryostats. In the dilution refrigerator, a calibrated carbon resistor

was mounted on the mixing chamber. In addition, nuclear orientation thermometry was used below 100 mK, with a Co crystal mounted on the sample holder adjacent to the sample.

Most of the work described here was done on a single copper crystal (used previously in Ref. 9) of nominal 99.999% Cu purity. This sample had a residual resistivity ratio (r_R) of 4000 and was oriented with its $\langle 110 \rangle$ axis normal to its surface. The sample was approximately 2 cm in diameter. In the dilution refrigerator, only $\frac{1}{2}$ of the sample was used. (It had been cut into four pieces using spark erosion). A polycrystalline sample of ultrahigh purity (r_R=18 000) copper was used in some of the lowest-temperature runs. This sample had been used previously in experiments by Kadono *et al.*[11,12] A small amount of material was cut from the 5-mm-diam sample rod and arranged to form a mosaic, covering an area of 30×20 mm^2. Although the sample was polycrystalline, the various crystallites were clearly visible in the freshly cut surfaces and were several millimeters in size.

VI. RESULTS

A. Level-crossing resonance: Quadrupolar interaction

The easiest and fastest way to detect any LCR's is by using time-integral μSR. The results of such an experiment are shown in Fig. 5 for muons in the copper single crystal in longitudinal fields from 0 to 120 G at two different temperatures. The location of the resonance (maximum asymmetry loss other than as $B \to 0$) around 80 G is evident, as is the width of the resonance and the difference between nearly static and diffusing muons. Since an exact theoretical model for the relaxation function was available, we chose to determine the strength of the copper quadrupolar interaction with the EFG of the
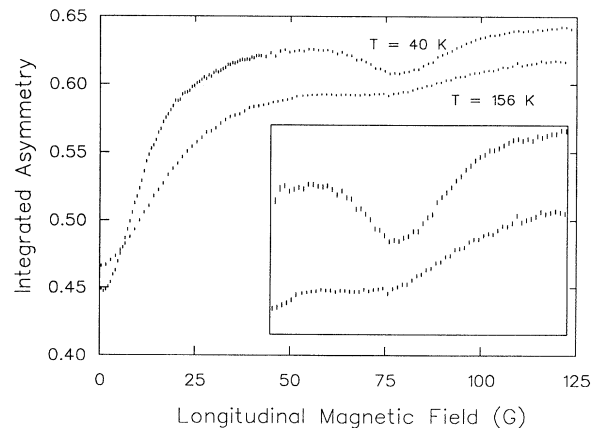
FIG. 5. Integral-μSR measurement of longitudinal relaxation. Field applied along the $\langle 110 \rangle$ direction. Inset: expanded vertical scale.

muon, using time-differential μSR.

We were able to accurately measure both the magnitude and sign of the quadrupole interaction, which had previously been reported[3] to be $\mid \omega^Q \mid = 3.02 \pm 0.4\ \mu s^{-1}$. This was done by collecting a series of spectra at the minimum in the hop rate around $T = 45$ K, in longitudinal fields where there was the maximum relaxation, as well as halfway down the resonance curve, both above and below the center of the resonance. The fields used were 70.1, 79.5, and 86.9 G. These runs were then simultaneously compared to theoretical functions calculated as described above for various values of the quadrupolar frequency ω^Q. A typical fit is shown in Fig. 6 for the three applied fields at $T = 50$ K. Other than normalizations between counters (constant for each of the three runs), the only free parameter was the quadrupolar frequency. Although both positive and negative signs for the quadrupolar frequency give a resonance at approximately 80 G (corresponding to $\omega_\mu^Z \approx \pm 2\omega^Q$), the resonance is asymmetric about its center and the total amplitude is slightly larger for the case of negative sign. This asymmetry is a result of the fact that the resonance does not occur exactly at $\omega_\mu^Z = \pm 2\omega^Q$, but is split into (unresolved) lines by the copper nuclear Zeeman interaction. The intensities of these various line (and thus the overall line shape) depend upon the relative orientation of the applied field and the muon-nuclear axis as well as the relative signs of the quadrupolar, Zeeman, and dipolar frequencies.

We found that it was only possible to fit the data by using a negative sign for the quadrupolar frequency; it was not possible to get a large enough amount of relaxation using the positive sign. This could not be an effect of hopping; even assuming the muon to be completely static, there was not enough amplitude in the theoretical resonance for the positive sign case—and slow hopping serves to *diminish* the amplitude of the resonance, as can be seen in Fig. 5.
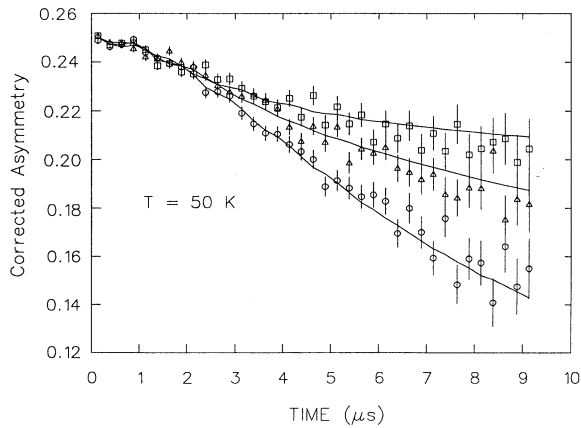
FIG. 6. Time-differential spectra around level-crossing resonance. Longitudinal fields are 70.1 (triangles), 79.5 (circles), and 86.9 G (squares).

Our final result for the quadrupolar frequency is

$$\omega^Q = -3.314(7)\ \mu s^{-1} = \frac{e^2 q Q}{4\hbar}. \qquad (31)$$

From this result, we can extract the electric-field gradient q. As the values of the copper quadrupole moments are slightly different, we use a weighted average for the two Cu isotopes. Effenberger *et al.*[32] give $|Q| = 0.220(15) \times 10^{-24}$ cm^2 for ^{63}Cu. Sternheimer[33] gives $Q = -0.209(5) \times 10^{-24}$ for ^{63}Cu and $Q = -0.194(4) \times 10^{-24}$ for ^{65}Cu. Using the average value of $Q = -0.205(5) \times 10^{-24}$ cm^2, we obtain

$$q = 0.296(7)\ \text{Å}^{-3}. \qquad (32)$$

This value may be compared with the theoretical result of Jena *et al.*,[34] who obtained $q = 0.26$ Å^{-3} for the EFG at copper nuclei due to an interstitial positive muon at the octahedral site (o site).

B. Muon site

The LCR data allow us to lay to rest the discussion of whether any of the apparent features observed at low temperatures are in fact due to a muon site change. If the muon were to change to another type of site or spend any significant time in some metastable site, such as the tetrahedral interstitial site (t site), there would be a change in the position of the level crossing. This is because the resonance position is given by the strength of the quadrupolar interaction of the nearest-neighbor copper atoms. A different site would be characterized by a different electric-field gradient, shifting the resonance position. Additionally, the number of neighbors participating in the resonance would be different, changing the amount of polarization involved in the resonance.

Time-differential measurements were made at a series of longitudinal fields around the LCR position at 10 mK. It was found that all of these runs could be fit simultaneously using the value of the hop rate extrapolated from Fig. 10 to 10 mK. The only free parameters were the asymmetry and α.

We see no evidence of any significant occupation of the tetrahedral site. Recalling that Flik *et al.*[35] and Seeger[36] reported metastable occupation by π^+'s of the tetrahedral site at $T = 150$ K, we can reconcile these two seemingly contradictory observations. The pion has a much shorter lifetime than the muon; therefore the muon would have to hop a factor of ~ 1000 more slowly than the pion, for a similar occupation of the metastable site to be equally apparent. Since they have similar masses and the same charge, we would, however, expect the muon and pion diffusion rates to be similar. Thus we conclude that the muon is never hopping infrequently enough in the temperature range available to us to observe possible occupation of such a metastable site.

It should be pointed out that the LCR is quite insensitive to small hop rates. The fact that the resonance does not quickly disappear due to hopping can be un-

derstood by considering the effect of hopping in longitudinal field. After a hop, the component of the muon polarization, which is perpendicular to the net field (random local field and applied longitudinal field), precesses. This perpendicular component is lost from the longitudinal polarization. After each hop to a different site with a different random field, this component is again lost and so on, as the total polarization is gradually relaxed away. This process only causes relaxation when there is hopping and is therefore quite sensitive to the magnitude of the hop rate. On the other hand, in the situation of the LCR, the muon polarization is lost through the resonant exchange with neighboring copper nuclei. Even if the muon is static, it is constantly losing polarization (even after five muon lifetimes), whereas in weak longitudinal field the situation is quickly reached where there is no further loss of polarization with time until the muon hops again (in the long-time tail). On resonance, the muons are constantly being depolarized, regardless of whether or not they are hopping. As a result, one would not expect the relaxation function around the LCR to be especially sensitive to the hop rate.

We have observed the LCR at temperatures up to 200 K, where the muon is hopping at a rate of approximately 1.5 μs^{-1}. The amplitude of the resonance at that temperature is slightly greater than expected on the basis of the strong collision model. This follows from the violation of the assumption that the hop rate is smaller than the dominant (in this case quadrupolar) spin interaction of the copper nuclei. In the field region away from the LCR, the second moment of the relaxation is different, depending on whether there is a strong or weak quadrupolar interaction. As the hop rate approaches the quadrupolar frequency, the quadrupolar interaction begins to be averaged out, causing a transition from the strong to the weak quadrupolar limit. As this happens, the second moment of the relaxation increases. Around the LCR, half of the main diagonal elements of the Hamiltonian are much smaller than away from the resonance; the hop rate approaches the magnitude of those elements much more quickly. The effective dipolar coupling (which gives the second moment) is then stronger, increasing the amount of relaxation. This acts to oppose the reduction of the resonance amplitude with hopping. The net result is that the hop rate that would be extracted on resonance by assuming $\omega^Q \gg \nu_{\text{hop}}$ is smaller than the actual value of ν_{hop}. As a result, the level-crossing persists to higher hop rates than predicted by the strong collision model.

C. Hop rate

In measuring the muon hop rate in copper, we used the weak-longitudinal-field (WLF) technique.[18,19] This technique has a number of advantages over both the transverse field and zero-field methods in determining hop rates.

As previously mentioned, the first transverse field results were subject to a number of alternate interpreta-

tions for the change in the relaxation rate at low temperature, including the muon site changing to one of different symmetry and trapping at defects. Transverse field measurements also suffered from a lack of sensitivity to changes in hop rate at very low hop rates. There is an additional difficulty in distinguishing the effects of small hop rates from the effects of a small ($\leq$ 5%) lattice dilation. In transverse field, many different physical interactions affect the amount of spin relaxation, often in ways that are virtually indistinguishable from each other.

Zero-field measurements of the hop rate are difficult near the minimum in the hop rate due to the fact that the decay of the "$\frac{1}{3}$ tail" does not show much effect until long times ($t \geq 8$ μs), where there are few muons still remaining in the sample. This problem is most pronounced at a "continuous" beam facility, such as TRIUMF, where one is limited to an optimum incoming muon rate by the requirement that only one muon be present in the sample at a time. This rate decreases as one observes out to longer times following the arrival of each muon. A further limitation of the ZF method is that the $\frac{1}{3}$ tail does not actually exist; the muon polarization does in fact decay slightly at long times, even when the muons are static.[15] If one used the approximate Kubo-Toyabe theory for the static muon polarization function, this would cause one to overestimate the hop rate. This is a less significant difficulty now that the exact solution for the static polarization function can be calculated, but it does demonstrate the sensitivity of results obtained in zero field to the fine details of the assumed static relaxation behavior.

The application of a longitudinal field increases the amount of polarization that is available to relax (due to hopping) from its approximate $\frac{1}{3}$ value in ZF, increasing the sensitivity of the WLF technique. In longitudinal field, the decay of the long-time tail begins at earlier times, where there are correspondingly more muons and any instrumental systematic distortions of the time spectra are smaller and therefore less significant. This is illustrated in Figs. 3 and 4, which show theoretical static and dynamic relaxation functions for both zero field and 15 G longitudinal field. The WLF polarization functions exhibit more significant differences at earlier times than do the zero-field functions. This increases the accuracy with which one can extract information from the data, since the error associated with any measurement of the polarization function increases exponentially with the time at which it is studied, due to the decreasing number of muons left in the sample.

At each temperature a series of spectra were taken at several applied longitudinal fields. Generally these fields were 8, 16, and 24 G. Typical spectra are shown in Figs. 7 and 8 where the muons are nearly static and diffusing rapidly, respectively. There are a number of advantages in taking a series of runs at various fields at each temperature. First, analyzing data for a number of different fields with all free parameters common to all the runs (i.e., hop rate, asymmetry, etc.) gives added confidence that one has a correct functional form and interpretation
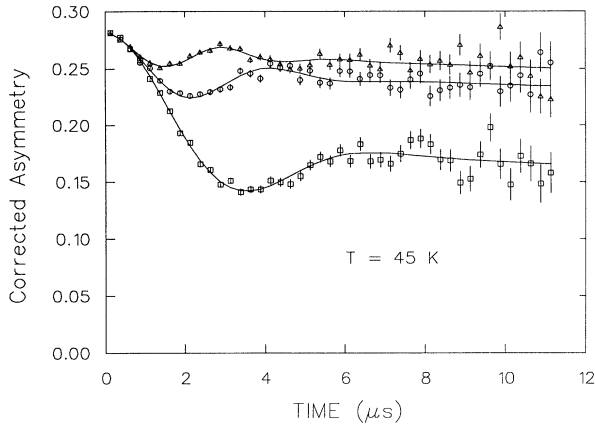
FIG. 7.   WLF time-differential μSR spectra for applied fields 8 (squares), 16 (circles), and 24 G (triangles). Muons are nearly static: T=45 K.

of the relaxation functions. Second, data at a series of fields extends the advantage that the WLF method has over zero field in that the field can be chosen such that one is most sensitive to small changes in ν_{hop}. This can be seen most clearly by referring to Fig. 9, which shows theoretical relaxation functions for various hop rates in zero field and in a longitudinal field of 15 G. It can be seen that there is a range of hop rates where the relaxation functions are not very sensitive to small changes in the hop rate, around the "T_1 minimum."[37] The hop rate where this takes place is field dependent. Using a series of fields guarantees that at worst one field will suffer from this lack of sensitivity.

The experimental asymmetry of the apparatus was determined in two ways. Transverse field spectra, taken by applying a field perpendicular to the direction in which

the longitudinal field was applied, provided one measure of the asymmetry. Furthermore, in fitting the WLF runs themselves, the asymmetry was fit. The results were always consistent with each other.

At this point the spectra were fit simultaneously (data from all three fields) using the MINUIT χ^2-minimization program. The only free parameters in these fits were the asymmetry, the relative efficiencies of the two counters, and the hop rate. The results obtained in these fits were also consistent with the results from fitting the runs separately. In a series of spectra at different temperatures taken under otherwise identical experimental conditions, the data were often fit simultaneously. For example, the points marked by diamonds in Fig. 10, taken at ten different temperatures and representing thirty different spectra, were fit together in a single global fit. The curves drawn through the data in Figs. 7 and 8 are typical of the fits obtained.

The relaxation functions used for fitting the LF data were calculated assuming the values of the μ^+-Cu dipolar interaction appropriate to the case where there is no lattice dilation, using the average gyromagnetic ratio $\gamma_{Cu}/2\pi = 1.154$ kHz/G for the two isotopes. The dipolar frequency was
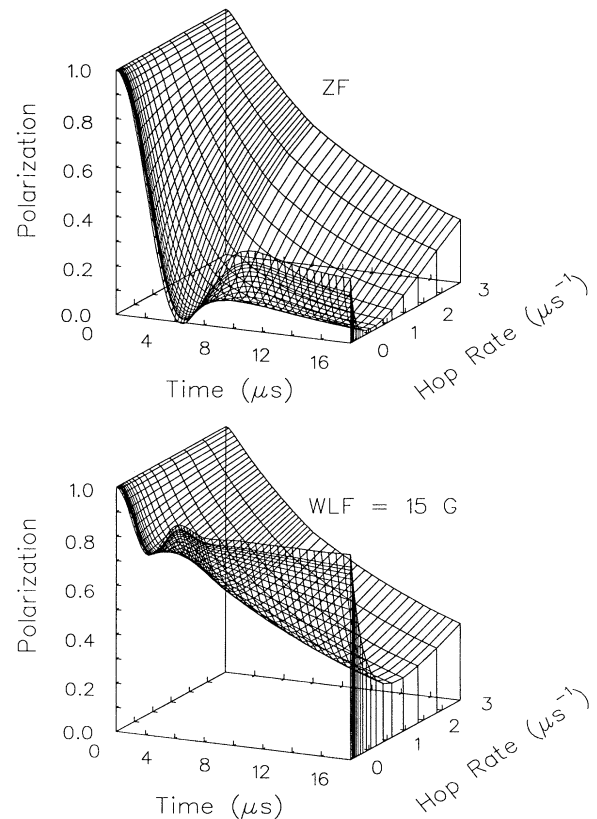
FIG. 9.   Dynamic relaxation functions in ZF and 15 G longitudinal field, as a function of muon hop rate ν_{hop} between 0 and 3 μs^{-1}.

FIG. 8.   WLF time-differential μSR spectra for applied fields 8 (squares), 16 (circles), and 24 G (triangles). Muons are diffusing rapidly: T=150 K.

$$\omega^D = 0.11 \ \mu\mathrm{s}^{-1} = \frac{\hbar\gamma_\mu\gamma_{\mathrm{Cu}}}{r^3_{\mathrm{Cu}-\mu}}. \tag{33}$$

This was calculated for a muon-copper distance of one half of the copper fcc lattice constant of 3.62 Å. The possible effects of lattice dilation were allowed in the fitting procedure through the use of a parameter that scaled the time axis, giving the first-order effect of a lattice dilation on the relaxation function. The fitted value of the parameter was 1.00(5) implying that any lattice dilation is less than 2%.

The second moment of the numerically computed relaxation functions may be obtained by numerical differentiation giving an effective $\Delta = 0.387 \ \mu\mathrm{s}^{-1}$, which can be compared to the experimental results of Clawson *et al.*,[9] $\Delta = 0.389(3) \ \mu\mathrm{s}^{-1}$, and Kadono and co-workers,[12,11] $\Delta = 0.390(1) \ \mu\mathrm{s}^{-1}$. These results are also clearly inconsistent with a 5% lattice dilation, which would give a significantly different value for Δ.

In interpreting this discrepancy between our results and the previous transverse field results (which reported a 5% dilation),[3] we note that the previous measurements were made at 20 and 80 K. Since the same results were obtained at the two temperatures, it was assumed that the muons were static. In fact, as can be seen in Fig. 10, these two temperatures happen to be on opposite sides of the minimum in the hop rate; the muons are hopping at about 0.06 $\mu\mathrm{s}^{-1}$. If the effect of this small hop rate is included in the calculation of the TF linewidth, an upper limit of approximately 2% is obtained for the lattice dilation.[38]

The quadrupolar frequency ω^Q was held fixed at $-3.2 \ \mu\mathrm{s}^{-1}$ for the hop rate analysis. The fact that this value is slightly different than the value eventually extracted for the quadrupolar frequency [given in Eq. (31)] from the analysis of the level crossing is unimportant,
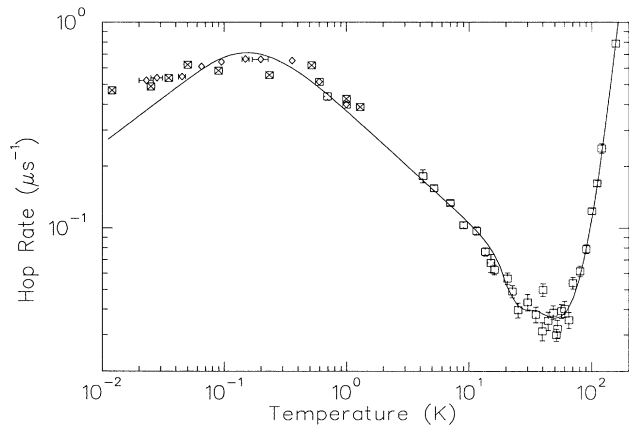
as the relaxation functions in fields away from the LCR are quite insensitive to the magnitude of the quadrupole splitting, so long as it is significantly greater than the Zeeman splitting.

The extracted hop rates have been fit in terms of Kondo's model for the diffusion rate of the muon as a function of various parameters that characterize the microscopic hopping Hamiltonian. Since the calculation of the hop rate in terms of these parameters requires reasonably intensive computations, the fitting was performed in stages. First, the region where the hop rate follows a $T^{-\alpha}$ relation was fit to extract a value of the coupling constant K ($\alpha = 2K - 1$). This value was then held fixed throughout the remaining analysis.

Following this, a series of theoretical hop rates were computed as a function of the remaining parameters, with the exception of the residual broadening δ_E, which was held to zero:

$$W = \frac{\mathcal{J}_0^2}{\Theta_D} \Xi\left(\frac{T}{\Theta_D}, S, \frac{\varepsilon_F}{k_B\Theta_D}, d, 0\right). \tag{34}$$

These results were stored in a multidimensional table, and a MINUIT fit was performed to extract results for the parameters in the temperature range above 500 mK. Finally, the effects of broadening were taken into account, and the value of δ_E necessary to provide the turning over in the hop rate below 500 mK was extracted.

The fitted hop rates are shown in Fig. 10 over the temperature range 12 mK < T < 150 K. It can be seen in Fig. 10 that there are a number of temperature regions exhibiting different hop rate behavior.

At the highest temperatures studied, 40 K< T <150 K, the muon diffuses by through-the-barrier phonon-assisted tunneling. The dominant process is that involving two phonons. The role of the phonons is to bring the energy levels between the two self-trapped states (before and after hopping) into coincidence, allowing a tunneling transition. We did not extend the study to higher temperatures, as the muon diffuses so rapidly that the strong collision model no longer gives accurate results for the hop rate (as discussed earlier). At such high rates, the most reliable method for deducing hop rates is through the use of high transverse fields.

In the intermediate temperature range there is a minimum in the hop rate in the crossover region between where the interactions of the muon with the lattice and with the conduction electrons dominate. Around this temperature range, we see the effect of the quadratic muon-lattice interaction, which causes a deepening of the minimum in the hop rate.

At lower temperatures 1.0 K< T <10 K, the hop rate increases with decreasing temperature. In this region, the hop rate has a power-law temperature dependence $\nu_{\mathrm{hop}} \sim T^{-\alpha}$. We extract a value of 0.553(7) for the exponent α. In terms of the predicted temperature dependence of Kondo and Yamada, the parameter $K = 0.224(4)$.

If we consider Yamada's result for the electron-muon coupling parameter K (assuming s-wave scattering of the

FIG. 10. Muon hop rate over the temperature range 12 mK< T <150 K. Squares and diamonds are for copper single crystal (r_R=4000). Crosses are for a high-purity (r_R=18 000) polycrystal. The curve is a fit to Kondo's model for muon diffusion with the parameters in Table I.

muon by electrons) given by

$$K = \frac{2}{\pi^2} \left(\tan^{-1} \frac{\sqrt{1-x}\tan\delta}{\sqrt{1+x\tan^2\delta}} \right)^2,$$

(35)

we can estimate a theoretical value for K. The phase shift δ is given by the Friedel sum rule in terms of the screened charge ($Z = 1$ in the case of the muon)

$$Z = \frac{2}{\pi} \sum_l (2l+1)\delta_l.$$

(36)

In the case where the muon is screened by electrons with s character ($l = 0$), we have $\delta = \frac{\pi}{2}$. The value of $x = J_0^2(k_F b)$ can be calculated using $k_F = 1.36\times10^8 \text{cm}^{-1}$ and $b = a/\sqrt{2}$, where $a = 3.62 \times 10^{-8}\text{cm}$ is the fcc lattice constant and J_0 is a spherical Bessel function. This gives an estimate of 0.28 for K, which is close to our measured value. The difference between the two values is presumably due to deviations from s character in the screening electron cloud. Hartmann et al.[39] interpolated the results of Puska and Nieminen,[40] who calculated the Fermi-level phase shifts for atoms in a homogeneous electron gas, obtaining $K = 0.33$ for copper and $K = 0.27$ for aluminum. Their experimental value for aluminum was $K = 0.15$. The smaller value for K is a result of aluminum's greater electron density relative to copper.

Below $T = 500$ mK, the value of the hop rate turns over and starts to decrease with decreasing temperature. This effect is explained by Kondo in terms of a phenomenologically introduced broadening of the energy levels before and after hopping. One possible source of this broadening in the case of copper could be the $^{63}\text{Cu}/^{65}\text{Cu}$ isotope mixture, where the site energy could depend on the number of each type of neighbor. As a result of this residual broadening, the hop rate no longer increases with decreasing temperature, but rather turns over at a temperature that corresponds roughly to the size of the residual broadening. Below this turnover, Kondo predicts that the hop rate will follow a T^{2K} temperature dependence. We find a weaker temperature dependence in the temperature range studied. Sugimoto[41] has also considered the effects of a distribution of final states that remains in the limit $T \to 0$. He finds the same results as Kondo when the occupation probability of sites reaches thermal equilibrium. In the opposite limit, where the site occupation probability is independent of the various site energies, he finds that the hop rate becomes temperature independent. Thus, one would expect the exponent in the hop rate to fall in the range $0 < \alpha < 2K$ below the turnover. One additional possible explanation for the discrepancy in the measured temperature dependence could be the existence of a range of residual broadenings, depending for example on the distance from impurities or dislocations. As a result, at lower temperatures (e.g., lower than all of these residual broadening energies) the hop rate might

TABLE I. Parameters extracted from hop-rate results, for Kondo's model for the muon hop rate.

J_0	37.1 ± 2.6 K
Θ_D	184.6 ± 2.0 K
ϵ_F/Θ_D	340.0 ± 20.0
S	7.15 ± 0.1
K	0.224 ± 0.004
d	171.1 ± 2.4
δ_E	0.37 K
$J_{\text{eff}} = e^{-S}J_0$	0.029 K

decrease more quickly.

The full results in terms of the various coupling parameters in Kondo's model are given in Table I. As can be seen, reasonable values of the various physical parameters are sufficient to fit our experimental results. The errors quoted are the statistical errors only and do not include any systematic uncertainties. Presumably, the actual uncertainties are somewhat larger. The value of $\Theta_D = 185$ K is in reasonable agreement with accepted results from heat capacity measurements (315 K), when it is considered that Θ_D only enters the calculations for the hop rate as an effective cutoff in the phonon spectrum. We note that the large value of the linear lattice coupling $S = 7.15$ implies a rather strong coupling of the muon to the lattice. As previously discussed, our estimate for the lattice dilation caused by the muon is less than 2%. Unfortunately, there is no straightforward method to determine whether these results are in conflict.

The temperature where the turnover takes place agrees well with the results previously reported by Kadono and co-workers,[12,11] who observed only a leveling off in the hop rate. We note, however, that the slope we extract is quite small. The fact that they were only able to measure down to $T = 69$ mK and that the zero-field technique is inherently less sensitive than the WLF method employed here may explain the fact that they were only able to observe the leveling off.

In comparing our results with those previously reported by Kadono and co-workers, we note that the greatest difference appears in the temperature range near the minimum in the hop rate. Their results are consistent with zero hopping at the minimum, whereas we report a minimum hop rate of ~ 0.03 μs^{-1}. The source of this discrepancy may lie with their use of a pulsed muon beam. Following a pulse, there are a number of distortions that affect the spectra. The early time region is distorted by beam positrons that scatter from the sample into the forward counter. This distortion was severe enough to force the discarding of the forward spectra.

Second, since all of the muons enter at once, the instantaneous positron counting rate just following a pulse is large enough that there is some counting inefficiency in the detectors. This problem was addressed by nu-

merically correcting the spectra for this counting loss. Typically, differences in the spectra before and after this correction were $\sim 1\%$, which is certainly significant relative to the precision of these experiments. They note[12,11] that these corrections tend to emphasize the static character of the relaxation functions.

Finally, most of the previous experiments were performed using backward decay muons. Such a beam contains rather higher-energy muons, and it is impossible to reject (and difficult to prevent) events originating from muons stopping outside of the sample. Any muons that stop in the aluminum sample holder or cryostat walls will provide a nonrelaxing background signal, which will also tend to indicate that the diffusion rate is lower than is actually the case (through the appearance of a long-lived tail).

Experiments with a "continuous" surface muon beam such as those reported here avoid these difficulties. Instantaneous beam rates in time-differential experiments are never high enough that the counting efficiency varies significantly and most of the beam positrons are removed through the use of a dc separator. The small beam spot of the surface beam helps ensure that most of the beam stops in the sample. The further requirement that each positron be correlated with an incident muon (which has entered through the thin muon counter) ensures that the detected positron came from a muon inside the sample.

VII. CONCLUSIONS

In conclusion, we have studied the diffusion of positive muons in copper between 12 mK and 150 K. We have shown that the changes in the muon relaxation function at various temperatures are due to muon diffusion rather than to site changes. In addition, we have measured the strength of the electric-field gradient exerted by the muon on its neighboring copper nuclei using the technique of level-crossing resonance. We find that the recent theories of Kondo, Yamada, and others for the quantum diffusion of light interstitials in metal give a good description of the temperature dependence of the muon diffusion rate, showing the importance of the conduction electron cloud in the diffusion process.

The source of the residual energy broadening seen below 500 mK is not completely clear although it seems that the isotopic mixture in natural copper may provide the necessary disorder. Further experiments on isotopically enriched samples of copper would be necessary to clarify this.

*Present address: Dept. of Physics, Columbia Univ., 538 West 120th St., New York, NY 10027.

†Present address: Dept. of Physics, Univ. of Alberta, Edmonton, Canada.

‡Present address: Dip. dell'ambiente, SEPA, CH-6500 Bellinzona, Switzerland.

§Present address: Riken 2-1 Hirosawa, Wako-shi, Saitima 351-01, Japan.

[1] I. I. Gurevich, E. A. Mel'eshko, I. A. Muratova, B. A. Nikol'sky, V. S. Roganov, V. I. Selivanov, and B. V. Sokolov, Phys. Lett. **40**, 143 (1972).

[2] V. G. Grebinnik, I. I. Gurevich, V. A. Zhukov, A. P. Manych, E. A. Meleshko, I. A. Muratova, B. A. Nikol'skii, V. I. Selivanov, and V. A. Suetin, Zh. Eksp. Teor. Fiz. **68**, 1548 (1975) [Sov. Phys. JETP **41**, 777 (1975)].

[3] M. Camani, F. N. Gygax, W. Ruegg, A. Schenck, and H. Schilling, Phys. Rev. Lett. **39**, 836 (1977).

[4] O. Hartmann, L. O. Norlin, A. Yaounac, J. Le Hericy, E. Karlsson, and T. O. Niinikoski, Hyperfine Interact. **8**, 533 (1981).

[5] J-M. Welter, D. Richter, R. Hempelmann, O. Hartmann, E. Karlsson, L. O. Norlin, T. O. Niinikoski, and D. Lenz, Z. Phys. B **52**, 303 (1983).

[6] J. M. Welter, D. Richter, R. Hempelmann, O. Hartmann, E. Karlsson, L. O. Norlin, and T. O. Niinikoski, Hyperfine Interact. **17-19**, 117 (1984).

[7] O. Echt, H. Graf, E. Holzschuh, E. Recknagel, A. Weidinger, and Th. Wichert, Phys. Lett. A **67**, 427 (1978).

[8] T. Natsui, T. Hatano, Y. Suzuki, R. Yamamoto, M. Doyama, K. Nishiyama, J. Imazato, and K. Nagamine, Phys. Lett. A **93**, 137 (1983).

[9] C. W. Clawson, K. M. Crowe, S. E. Kohn, S. S. Rosenblum, C. Y. Huang, J. L. Smith, and J. H. Brewer, Physica **109**, 2164 (1982).

[10] R. Kadono, J. Imazato, K. Nishiyama, K. Nagamine, T. Yamazaki, D. Richter, and J. M. Welter, Hyperfine Interact. **17-19**, 109 (1984).

[11] R. Kadono, J. Imazato, T. Matsuzaki, K. Nishiyama, K. Nagamine, T. Yamazaki, D. Richter, and J.-M. Welter, Phys. Rev. B **39**, 23 (1989).

[12] R. Kadono, T. Matsuzaki, K. Nagamine, T. Yamazaki, D. Richter, and J. M. Welter, Hyperfine Interact. **31**, 205 (1986).

[13] R. Kubo and T. Toyabe, in *Magnetic Resonance and Relaxation*, edited by R. Blinc (North-Holland, Amsterdam, 1966), p. 810.

[14] R. S. Hayano, Y. J. Uemura, J. Imazato, N. Nishida, T. Yamazaki, and R. Kubo, Phys. Rev. B **20**, 850 (1979).

[15] M. Celio and P. F. Meier, Phys. Rev. B **27**, 1908 (1983).

[16] R. Kadono, J. Imazato, K. Nishiyama, K. Nagamine, T. Yamazaki, D. Richter, and J. M. Welter, Hyperfine Interact. **17-19**, 109 (1983).

[17] M. Camani, D. G. Fleming, F. N. Gygax, W. Ruegg, A. Schenck, and H. Schilling, Hyperfine Interact. **6**, 265 (1979).

[18] J. H. Brewer, M. Celio, D. R. Harshman, R. Keitel, S. R. Kreitzman, G. M. Luke, D. R. Noakes, R. E. Turner, E. J. Ansaldo, C. W. Clawson, K. Crowe, and C. Y. Huang, Hy-

perfine Interact. **31**, 191 (1986).

[19] J. H. Brewer, S. R. Kreitzman, K. M. Crowe, C. W. Clawson, and C. Y. Huang, Phys. Lett. A **120**, 199 (1987).

[20] K. W. Kehr, G. Honig, and D. Richter, Z. Phys. B **32**, 49 (1978).

[21] M. Celio, Phys. Rev. Lett. **56**, 2720 (1986); Hyperfine Interact. **31**, 41 (1986).

[22] S. R. Kreitzman, J. H. Brewer, D. R. Harshman, R. Keitel, D. L. Williams, K. M. Crowe, and E. J. Ansaldo, Phys. Rev. Lett. **56**, 181 (1986).

[23] R. F. Kiefl, M. Celio, T. L. Estle, S. R. Kreitzman, G. M. Luke, T. M. Riseman, and E. J. Ansaldo, Phys. Rev. Lett. **60**, 224 (1988).

[24] Y. J. Uemura, Master's thesis, University of Tokyo, 1979.

[25] M. Celio, Hyperfine Interact. **31**, 153 (1986).

[26] C. P. Flynn and A. M. Stoneham, Phys. Rev. B **1**, 3966 (1970).

[27] Yu. Kagan and M. I. Klinger, J. Phys. C **7**, 2791 (1974).

[28] J. Kondo, Physica **84B**, 40 (1984); **126B**, 377 (1984); Hyperfine Interact. **31**, 117 (1986).

[29] K. Yamada, Prog. Theor. Phys. **72**, 195 (1984); K. Yamada, A. Sakurai, S. Miyazima, and H. S. Hwang, *ibid.* **75**, 1030 (1986).

[30] A. Schenck, *Muon Spin Rotation Spectroscopy: Principles and Applications in Solid State Physics* (Hilger, Bristol, 1985); S. F. J. Cox, J. Phys. C **20**, 3187 (1987).

[31] For general aspects of muon-spin relaxation, see proceedings of four previous international conferences [Hyperfine Interact. **6** (1979); **8** (1981); **17-19** (1984); **31** (1986)].

[32] B. Effenberger, W. Kunold, W. Oesterle, M. Schneider, L. M. Simons, R. Abela, and J. Wüest, Z. Phys. A **309**, 77 (1982).

[33] R. M. Sternheimer, Phys. Rev. A **6**, 1702 (1972).

[34] P. Jena, S. G. Das, and K. S. Singwi, Phys. Rev. Lett. **40**, 264 (1978).

[35] G. Flik, J. Bradbury, W. Cooke, M. Leon, M. Paciotti, M. Schillaci, K. Maier, and A. Seeger, Hyperfine Interact. **31**, 61 (1986).

[36] A. Seeger, μSR Newslett. **34**, 1880 (1988).

[37] C. P. Slichter, *Principles of Magnetic Resonance* (Springer-Verlag, Berlin, 1978).

[38] M. Celio (private communication).

[39] O. Hartmann, E. Karlsson, E. Wäckelgård, R. Wäppling, D. Richter, R. Hempelmann, and T. O. Niinikoski, Phys. Rev. B **37**, 4425 (1988).

[40] M. J. Puska and R. M. Nieminen, Phys. Rev. **27**, 6121 (1983).

[41] H. Sugimoto, J. Phys. Soc. Jpn. **55**, 1687 (1986).